Polarization-insensitive unidirectional spoof surface plasmon polaritons coupling by gradient metasurface*

Hong-yu Shi(施宏宇)[1], An-xue Zhang(张安学)[1,2,†], Jian-zhong Chen(陈建忠)[1], Jia-fu Wang(王甲富)[3], Song Xia(夏颂)[4], and Zhuo Xu(徐卓)[4]

[1] *School of Electronic and Information Engineering, Xi'an Jiaotong University, Xi'an* 710049, *China*
[2] *Beijing Center for Mathematics and Information Interdisciplinary Science (BCMIIS), Beijing* 100048, *China*
[3] *College of Science, Air Force Engineering University, Xi'an* 710051, *China*
[4] *Electronic Materials Research Laboratory, Key Laboratory of the Ministry of Education, Xi'an Jiaotong University, Xi'an* 710049, *China*

(Received 25 January 2016; revised manuscript received 4 March 2016; published online 9 June 2016)

A polarization-insensitive unidirectional spoof surface plasmon polariton (SPP) coupler mediated by a gradient metasurface is proposed. The field distributions and average Poynting vector of the coupled spoof SPPs are analyzed. The simulated and experimental results support the theoretical analysis and indicate that the designed gradient metasurface can couple both the parallel-polarized and normally-polarized incident waves to the spoof SPPs propagating in the same direction at about 5 GHz.

Keywords: spoof surface plasmon polariton, metamaterials, gradient metasurfaces

PACS: 81.05.Xj **DOI:** 10.1088/1674-1056/25/7/078105

1. Introduction

Surface plasmon polaritons (SPPs) are propagating excitations generated by the coupling of light and electron density at the surface of a metal. SPPs can be manipulated by the structure of the surface at the subwavelength scale, which means that it plays an important role in optical technology[1–4] and nano-devices.[5–7] Actually, SPP-like modes or spoof SPPs are also observed at structured surfaces in the microwave frequency and have been applied to microwave cloaks,[8–11] waveguides,[12–14] and antennas.[15,16]

Metasurfaces are planar metamaterials with one- or two-dimensional arrangements of subwavelength resonators. Metasurfaces can manipulate the amplitude,[17–19] phase,[20,21] polarization,[22–25] and propagation direction of the electromagnetic waves including surface waves.[26–30] Over the past few years, considerable interest has been focused on metasurfaces with phase discontinuities or gradient metasurfaces. Different types of gradient metasurfaces have been designed to manipulate the propagation of electromagnetic waves in the frequency range from optics to microwave.[31–42] One- and two-dimensional gradient metasurfaces have been reported to realize anomalous reflection or refraction.[31–39] Also, when the phase gradient of the gradient metasurface is sufficiently large, the gradient metasurface can couple the normal incident electromagnetic waves to the spoof SPPs propagating along the direction of the phase gradient.[40–43]

Great efforts have been made to excite SPPs or spoof SPPs in a specific direction.[44–48] Cui *et al.* presented a holographic metasurface composed of unit cells with different surface impedances and dispersion properties to realize surface wave coupling.[48] A gradient metasurface is another efficient choice to generate unidirectional spoof SPPs. In terms of spoof SPP couplings by gradient metasurfaces, the subwavelength resonators of the gradient metasurface should have different reflection phases to realize an appropriate phase gradient that controls the wavelength and amplitude of the coupled spoof SPPs. In addition, the resonators of the gradient metasurface should have the same dispersion properties to offer the necessary phase-matching conditions to match the dispersion properties of the coupled spoof SPPs defined by the phase gradient.[43] While, the unit cells of the holographic metasurfaces could have different dispersion properties to manipulate the wavefront of the surface waves.[48]

Types of gradient metasurfaces have been carefully designed for spoof SPP coupling.[40–43] However, these designs are polarization sensitive or are realized by complex two-dimensional arranged structures.[49] Linearly polarized gradient metasurfaces are reported as spoof SPP couplers.[40,41] They can only couple the incident wave polarized in the phase gradient direction to spoof SPPs. Circularly polarized gradient metasurfaces have also been reported.[42,43] Generally, the efficiency of the circularly polarized gradient metasurfaces is polarization insensitive; however, the directions of the coupled spoof SPPs are polarization-controlled. This means that circularly polarized gradient metasurfaces couple electromagnetic waves with different helicity to spoof SPPs in opposite direc-

*Project supported by the China Postdoctoral Science Foundation (Grant No. 2015M580849) and the National Natural Science Foundation of China (Grant Nos. 61471292, 61501365, 61471388, 61331005, 41404095, and 41390454).

†Corresponding author. E-mail: anxuezhang@mail.xjtu.edu.cn

© 2016 Chinese Physical Society and IOP Publishing Ltd

tions. Also, the field distributions are only analyzed in situations where the incident wave is polarized in the phase gradient direction.[40] Thus, analysis of field distributions of the coupled spoof SPPs under different polarized incident waves and the development of polarization-insensitive unidirectional spoof SPP couplers are desirable.

In this article, we present a gradient metasurface with one-dimensional arrangements of subwavelength resonators supporting polarization-insensitive unidirectional spoof SPP coupling. Theoretical analysis of the situations with both gradient direction polarized incident wave and its cross-polarized incident wave is presented based on the generalized Snell law. The proposed gradient metasurface can couple arbitrary polarized electromagnetic waves at normal incidence to spoof SPPs propagating along the same direction at about 5 GHz. However, for different polarizations of the incident waves, the coupled spoof SPPs propagate in the same direction but with different modes. Thus, the coupled spoof SPPs preserve the polarization information of the incident wave and the proposed gradient metasurface has the potential to realize polarization analyzers.

2. Theoretical analysis

The subwavelength resonators of the gradient metasurfaces are each individually designed to tune the reflective phase and to realize a phase gradient. As shown in Fig. 1, the wavefronts of the electromagnetic waves can be manipulated in line with the generalized Snell law[36]

$$\sin\theta_{\rm r} - \sin\theta_{\rm i} = \frac{1}{n_{\rm i}k_{\rm i}}\frac{{\rm d}\Phi}{{\rm d}x}, \tag{1}$$

where $\theta_{\rm i}$ and $\theta_{\rm r}$ are the incident and reflection angles, respectively, $n_{\rm i}$ is the refractive index of the medium, ${\rm d}\Phi/{\rm d}x = \xi$ is the phase gradient along the x direction, and $k_{\rm i}$ is the wave number of the incident wave in free space. Following the generalized Snell law, in free space, the reflection angle satisfies the following equation:

$$\sin\theta_{\rm r} = \frac{k_{\rm r}^x}{k_0} = \frac{\xi}{k_0} + \sin\theta_{\rm i} = \frac{k_{\rm i}^x + \xi}{k_0}, \tag{2}$$

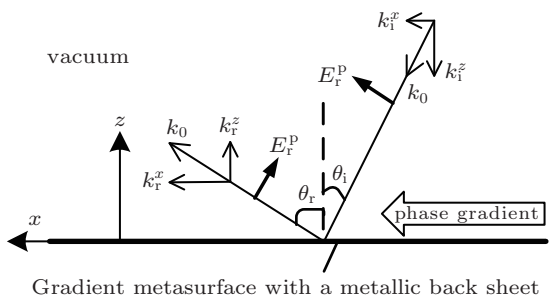


Fig. 1. Schematic illustration of a parallel-polarized field ($E_{\rm i}^{\rm p}$) incident onto a gradient metasurface. $E_{\rm r}^{\rm p}$ is the reflected field. The incident plane is the xz plane. The $k_{\rm i}^x$ and $k_{\rm i}^z$ are the wave vectors of the incident wave in the x and z directions, respectively. The $k_{\rm r}^x$ and $k_{\rm r}^z$ are the wave vectors of the reflected wave in the x and z directions, respectively.

where k_0 is the wave number in the vacuum. Thus, the wave number along the direction of the reflected wave can be written as $k_{\rm r}^x = \xi + k_{\rm i}^x$, where ξ is the phase gradient and $k_{\rm i}^x$ is the wave number of the incident wave in the x direction.

2.1. Analysis of parallel-polarized incident wave

As shown in Fig. 1, consider a parallel-polarized incident wave with electric field written as $\boldsymbol{E}_{\rm i}^{\rm p} = E_0(\cos\theta_{\rm i}\hat{\boldsymbol{x}} + \sin\theta_{\rm i}\hat{\boldsymbol{z}})\exp({\rm j}k_{\rm i}^x x - {\rm j}k_{\rm i}^z z)\exp(-{\rm j}\omega t)$, where ω is the frequency. According to the generalized Snell law, the reflected electric field is

$$\begin{aligned}\boldsymbol{E}_{\rm r}^{\rm p} &= \alpha E_0(-\cos\theta_{\rm r}\hat{\boldsymbol{x}} + \sin\theta_{\rm r}\hat{\boldsymbol{z}})\exp({\rm j}k_{\rm r}^x x + {\rm j}k_{\rm r}^z z)\exp(-{\rm j}\omega t)\\ &= \alpha E_0(-(k_{\rm r}^z/k_0)\hat{\boldsymbol{x}} + (k_{\rm r}^x/k_0)\hat{\boldsymbol{z}})\\ &\quad\times\exp({\rm j}k_{\rm r}^x x + {\rm j}k_{\rm r}^z z)\exp(-{\rm j}\omega t),\end{aligned} \tag{3}$$

where α is the reflection coefficient, k_0 is the wave number in the vacuum, and $k_{\rm r}^x$ and $k_{\rm r}^z$ are the wave numbers of the reflected wave along the x and z directions and satisfy $k_0^2 = k_{\rm r}^{x2} + k_{\rm r}^{z2}$ and $k_{\rm r}^x = k_{\rm i}^x + \xi \neq 0$. According to Maxwell's equations, the magnetic field of the reflected wave is

$$\boldsymbol{H}_{\rm r}^{\rm p} = -\hat{\boldsymbol{y}}\alpha E_0\exp({\rm j}k_{\rm r}^x x + {\rm j}k_{\rm r}^z z)\exp(-{\rm j}\omega t)/\eta_0, \tag{4}$$

where η_0 is the wave impedance of free space. When $k_{\rm r}^x > k_0$, $k_{\rm r}^z$ is purely imaginary, then the x and z components of the reflected electric field have a phase difference of 90°. The electric and magnetic fields can then be written as

$$\begin{aligned}\boldsymbol{E}_{\rm r}^{\rm p} &= \alpha E_0\exp(-|k_{\rm r}^z|z)[-({\rm j}|k_{\rm r}^z|/k_0)\hat{\boldsymbol{x}} + (k_{\rm r}^x/k_0)\hat{\boldsymbol{z}}]\\ &\quad\times\exp({\rm j}k_{\rm r}^x x)\exp(-{\rm j}\omega t),\end{aligned} \tag{5}$$

$$\begin{aligned}\boldsymbol{H}_{\rm r}^{\rm p} &= -\hat{\boldsymbol{y}}\alpha E_0\exp(-|k_{\rm r}^z|z)\exp({\rm j}k_{\rm r}^x x)\\ &\quad\times\exp(-{\rm j}\omega t)/\eta_0.\end{aligned} \tag{6}$$

Equations (5) and (6) indicate that the reflected wave is propagating in the x direction and is confined in the z direction. So, the incident wave is coupled to the spoof SPPs. The y component of the magnetic field has a $-90°$ phase difference to the x component of the electric field and a 180° phase difference to the z component of the electric field. The wavelength of the coupled spoof SPPs is

$$\lambda_{\rm sspp} = 2\pi/(k_{\rm i}^x + \xi). \tag{7}$$

Equation (7) indicates that the wavelength of the coupled spoof SPPs is controlled by the phase gradient. Also, with normal incidence ($k_{\rm i}^x = 0$), the wavelength of the coupled spoof SPPs is only controlled by the phase gradient and is, in principal, independent of the frequency of the incident wave (in practice the meta-atoms sill probably exhibit some frequency dependency).

2.2. Analysis of the normal-polarized incident wave

When the incident wave is a normal-polarized wave as shown in Fig. 2, the electric and magnetic fields of the incident wave are

$$\boldsymbol{E}_{\rm i}^{n} = -\hat{\boldsymbol{y}}\exp(\mathrm{j}k_{\rm i}^{x}x-\mathrm{j}k_{\rm i}^{z}z)\exp(-\mathrm{j}\omega t), \quad (8)$$

$$\boldsymbol{H}_{\rm i}^{n} = -E_0(\cos\theta_{\rm i}\hat{\boldsymbol{x}}+\sin\theta_{\rm i}\hat{\boldsymbol{z}})\exp(\mathrm{j}k_{\rm i}^{x}x-\mathrm{j}k_{\rm i}^{z}z) \times \exp(-\mathrm{j}\omega t)/\eta_0. \quad (9)$$

Similar to the condition with the parallel-polarized incident wave, when $k_{\rm r}^{x}=k_{\rm i}^{x}+\xi>k_0$, the electric and magnetic fields of the reflected wave are

$$\boldsymbol{E}_{\rm r}^{n} = -\hat{\boldsymbol{y}}\alpha E_0\exp(-|k_{\rm r}^{z}|z)\exp(\mathrm{j}k_{\rm r}^{x}x)\exp(-\mathrm{j}\omega t), \quad (10)$$

$$\boldsymbol{H}_{\rm r}^{n} = \alpha E_0[(\mathrm{j}|k_{\rm r}^{z}|/k_0)\hat{\boldsymbol{x}}-(k_{\rm r}^{x}/k_0)\hat{\boldsymbol{z}}] \times \exp(-|k_{\rm r}^{z}|z+\mathrm{j}k_{\rm i}^{x}x-\mathrm{j}\omega t)/\eta_0. \quad (11)$$

According to Eqs. (10) and (11), the z component of the reflected magnetic field is generated, and the normal-polarized incident wave can also be converted to spoof SPPs propagating in the x direction.

Consequently, both parallel-polarized and normal-polarized incident waves can be coupled to spoof SPPs propagating in the same direction, but in different modes. The parallel-polarized incident wave coupled spoof SPPs have a z component of the electric field, while the normal-polarized incident wave coupled spoof SPPs do not. Thus, the polarization state of the incident wave can be analyzed by detecting the z component of the electric field of the coupled spoof SPPs.

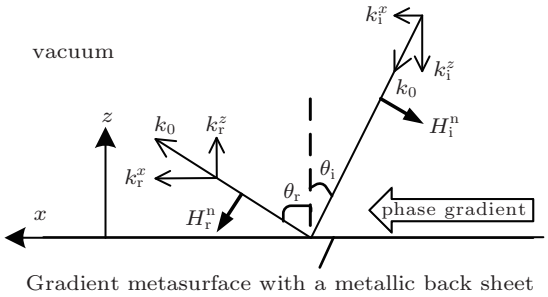


Fig. 2. Schematic illustration of a normal-polarized field incident onto a gradient metasurface. $H_{\rm r}^{\rm p}$ is the reflective field. The incident plane is the xz plane. The $k_{\rm i}^{x}$ and $k_{\rm i}^{z}$ are the wave vectors of the incident wave in the x and z directions, respectively. The $k_{\rm r}^{x}$ and $k_{\rm r}^{z}$ are the wave vectors of the reflected wave in the x and $z$directions, respectively.

3. Design of the gradient metasurface

To verify the above theoretical analysis, we designed a polarization-insensitive gradient metasurface as shown in Fig. 3. TACONIC CER-10 with a thickness of 3.18 mm ($0.053\lambda_0$, where λ_0 is the wavelength of the incident wave at 5 GHz in free space) was used as a substrate with a dielectric constant of 10 and a loss tangent 0.0035. The designed resonator (shown in Fig. 3(a)) consists of a metallic pattern and a back metallic sheet. As shown in Fig. 3(a), the outer structure is used to realize an electrically small resonator,[50] and the inner structure (Meander line) with a different geometric parameter l is used to tune the reflection phase of the resonator,[51] as shown in Fig. 3(b). Because of the back metallic sheet, the incident wave is almost totally reflected. Because the resonator is isotropic, the properties of the resonator are polarization insensitive.

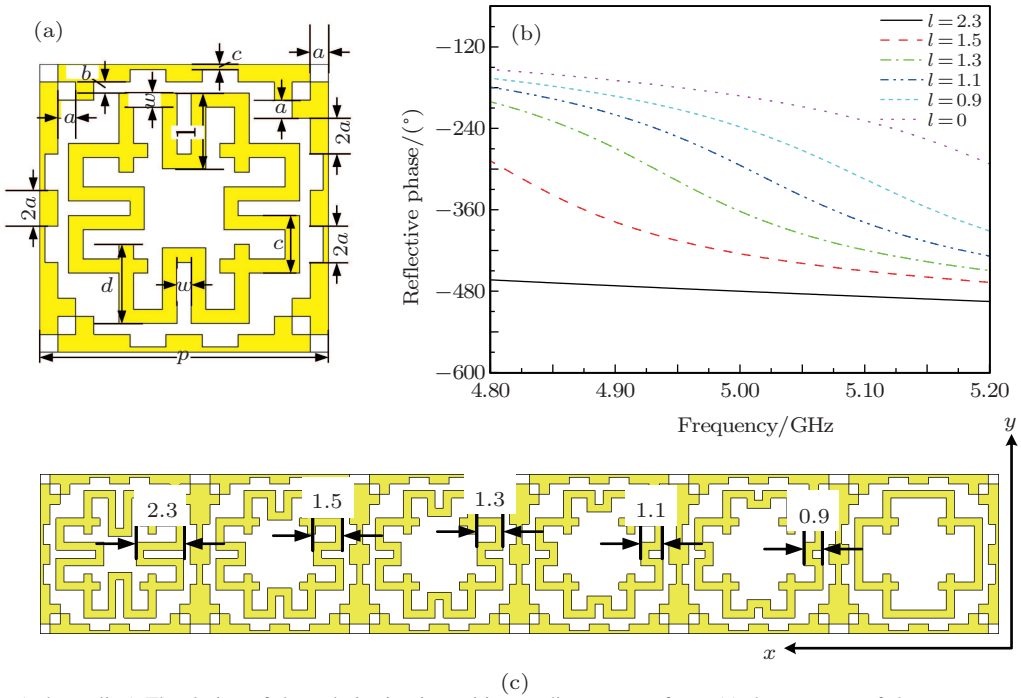


Fig. 3. (color online) The design of the polarization-insensitive gradient metasurface: (a) the structure of the resonator; (b) the reflective phase of the resonator with different l, and a phase change step of 60° was obtained; (c) the unit cell of the designed gradient metasurface.

The geometry of the structure was optimized by simulations. The geometric parameters of the resonator were chosen to be $a = 0.5$ mm, $b = 0.3$ mm, $c = 0.15$ mm, $d = 2.2$ mm, $e = 1.6$ mm, $w = 0.4$ mm, and $p = 8$ mm ($0.133\lambda_0$). The unit cell (shown in Fig. 3(c)) of the gradient metasurface is composed of six resonators in a one-dimensional arrangement along the x direction with $l = 0$ mm, 0.9 mm, 1.1 mm, 1.3 mm, 1.5 mm, and 2.3 mm. The reflective phase of each resonator was designed to obtain a phase change of 60° at 5 GHz, resulting in a phase gradient $\xi = 1.25k_0$ in the x direction on the interface. Thus, at 5 GHz, $k_0 < \xi$, and the incident wave can be coupled to spoof SPPs even at normal incidence ($k_i^x = 0$).

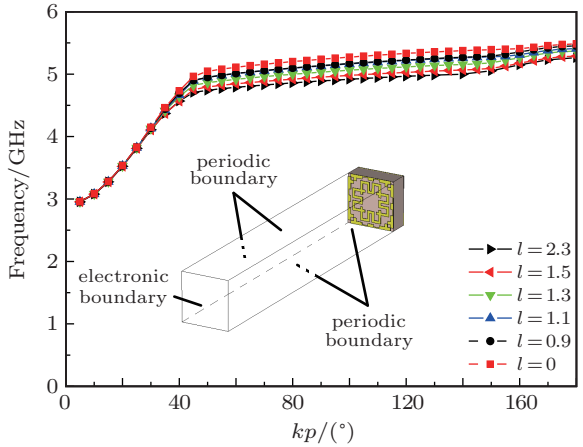


Fig. 4. (color online) The simulated dispersion curves of the resonators with different geometric parameter l. k is the wave number of the excitation and p is the period of the resonators.

The simulated dispersion curves of the subwavelength resonators in Fig. 3(a) with different geometric parameter l were obtained using the eigen mode solver of the commercial software CST MICROWAVE STUDIO, as shown in Fig. 4. The inserted figure shows the boundary conditions in the simulation. Periodic boundary conditions were set in the x and y directions, and an electric boundary was defined in the z direction. According to the theoretical analysis and Eq. (7), for the coupled spoof SPPs, $kp = \xi p = 60°$ in the proposed design at normal incidence. As shown in Fig. 4, when $kp = 60°$, the dispersion curves of the resonators with different l are approximately the same at around 5 GHz. This result matches the frequency where the phase gradient is realized as shown in Fig. 3(b) and satisfies the phase-matching condition. Thus, spoof SPP coupling can occur at about 5 GHz.

4. Simulation and measurement results

4.1. The simulation results

The designed gradient metasurface with unit cells shown in Fig. 3(c) was simulated by the commercial software CST MICROWAVE STUDIO. The periodic boundary conditions were set in the x and y directions. Floquet ports were used as excitations in the frequency range of 4.8–5.4 GHz in the z direction (Fig. 5). To demonstrate the spoof SPP coupling capability of the gradient metasurface, a wave at normal incidence illuminated the model. Because of $k_i^x = 0$, the incident plane is the xz plane, the x-polarized wave is parallel-polarized and the y-polarized wave is normal-polarized.

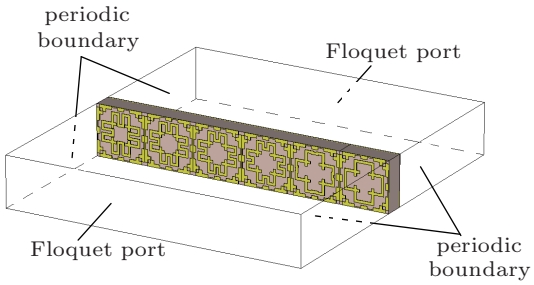


Fig. 5. (color online) Schematic of the simulation.

The simulated reflection coefficients are shown in Fig. 6. At 5.09 GHz, the reflectances of the parallel-polarized (R_{pp}) and normal-polarized (R_{nn}) incident waves are −13.7 dB and −15.3 dB, respectively. The cross-polarized reflections (R_{pn} and R_{np}) are below −20 dB. The differences between R_{pp} and R_{nn} are caused by the different arrangements of the resonators along the x and y directions. According to the theoretical analysis, the reflection dips at 5.09 GHz are caused by the polarization-insensitive spoof SPP couplings when $\xi > k_0$. The reflectance dip with parallel-polarized incidence at 4.87 GHz is caused by the properties of the designed resonators and the different arrangements of the resonators in the x and y directions. The parallel-polarized incident wave is also coupled to spoof SPPs propagating in the x direction at 4.87 GHz.

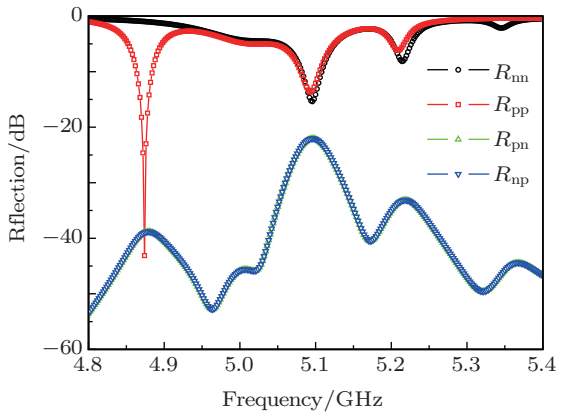


Fig. 6. (color online) The simulated reflectance of the designed gradient metasurface.

The simulated electromagnetic fields under parallel-polarized incident wave illumination at 5.09 GHz are shown in Figs. 7(a)–7(c). The x and z components of the total electric field are shown in Figs. 7(a) and 7(c), respectively. The surface-confined spoof SPPs are generated and are propagating in the x direction. Figure 7(d) shows the total power flow on the xz plane at 5.09 GHz under parallel-polarized incidence and indicates that the coupled spoof SPPs propagate along the x direction, and are evanescent and confined in the z direction.

To verify the above theoretical analysis, the phase of the coupled spoof SPPs is discussed. The z component of the electric field is induced and has a 90° phase difference to the x component of the electric field. The y component of the total magnetic field of the spoof SPPs has a $-90°$ phase difference to the x component of the electric field and a 180° phase difference to the z component of the electric field as shown in Fig. 7(b). The wavelength of the spoof SPPs is $2\pi/\xi = 6 \times p$.

For a normal-polarized (y-polarized) incident wave, the simulated electromagnetic fields and power flow are shown in Fig. 8. At 5.09 GHz, the simulated y component of the total electric field is shown in Fig. 8(a). The x and z components of the total magnetic field are shown in Figs. 8(b) and 8(c), respectively. Figures 8(a)–8(c) indicate that the coupled waves are condensed on the surface and are evanescent in the z direction. Thus, the normal-polarized incident wave is also coupled to the spoof SPPs. Figure 8(d) shows the total power flow in the xz plane at 5.09 GHz at normal-polarized incidence and indicates that the coupled spoof SPPs are propagating in the x direction, the same as the situation with parallel-polarized incidence.

The z component of the magnetic field is induced and has a 90° phase difference to the x component of the magnetic field. The y component of the electric field of the spoof SPPs has a $-90°$ phase difference to the x component of the magnetic field and a 180° phase difference to the z component of the magnetic field. The wavelength of the spoof SPPs is $6 \times p = 48$ mm. Thus, the simulated results are in agreement with Eqs. (10) and (11) and verify the theoretical analysis.

According to the above discussion, the properties of the simulated electromagnetic field agree well with the above theoretical analysis and demonstrate the spoof SPP coupling capability of the designed gradient metasurface. Since an arbitrary polarized wave can be decomposed into a parallel-polarized wave and a normal-polarized wave, the designed gradient metasurface can couple an arbitrary polarized wave to spoof SPPs propagating in one direction (the x direction, or the phase gradient direction).

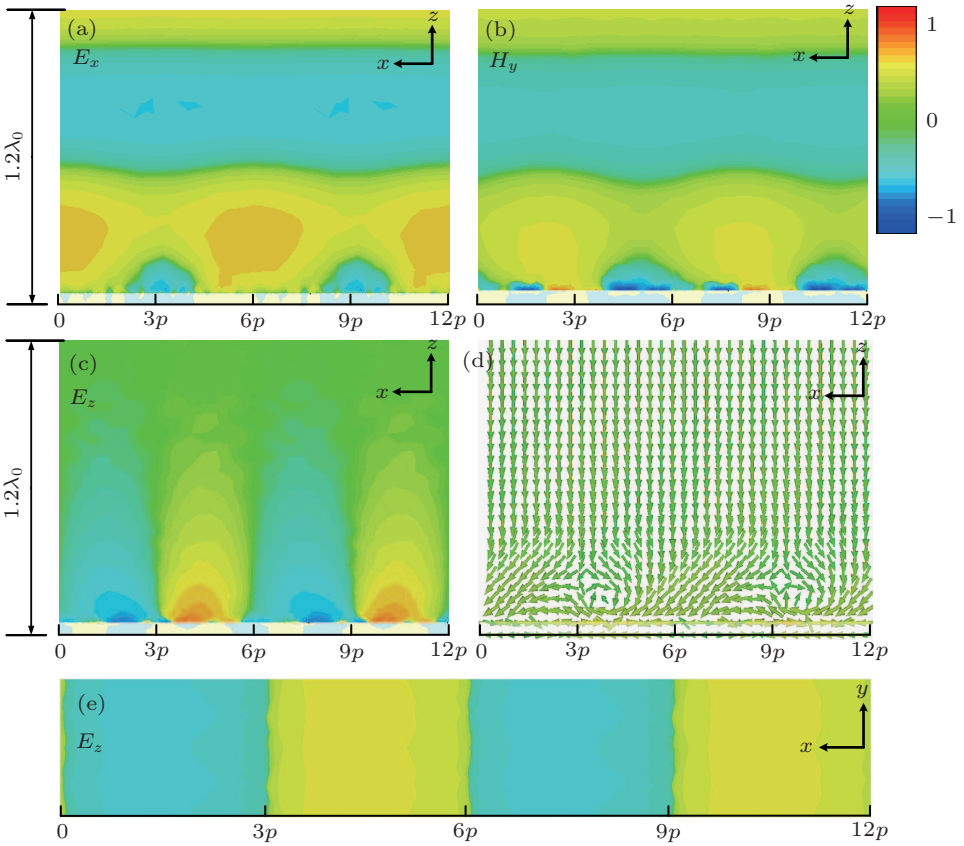


Fig. 7. (color online) (a) The x component of the total electric field. (b) The y component of the total magnetic field. (c) The z component of the total electric field in the xz plane. (d) The total power flow in the xz plane at 5.09 GHz under parallel-polarized incidence. (e) The z component of the total electric field in the xy plane at $z = 5$ mm.

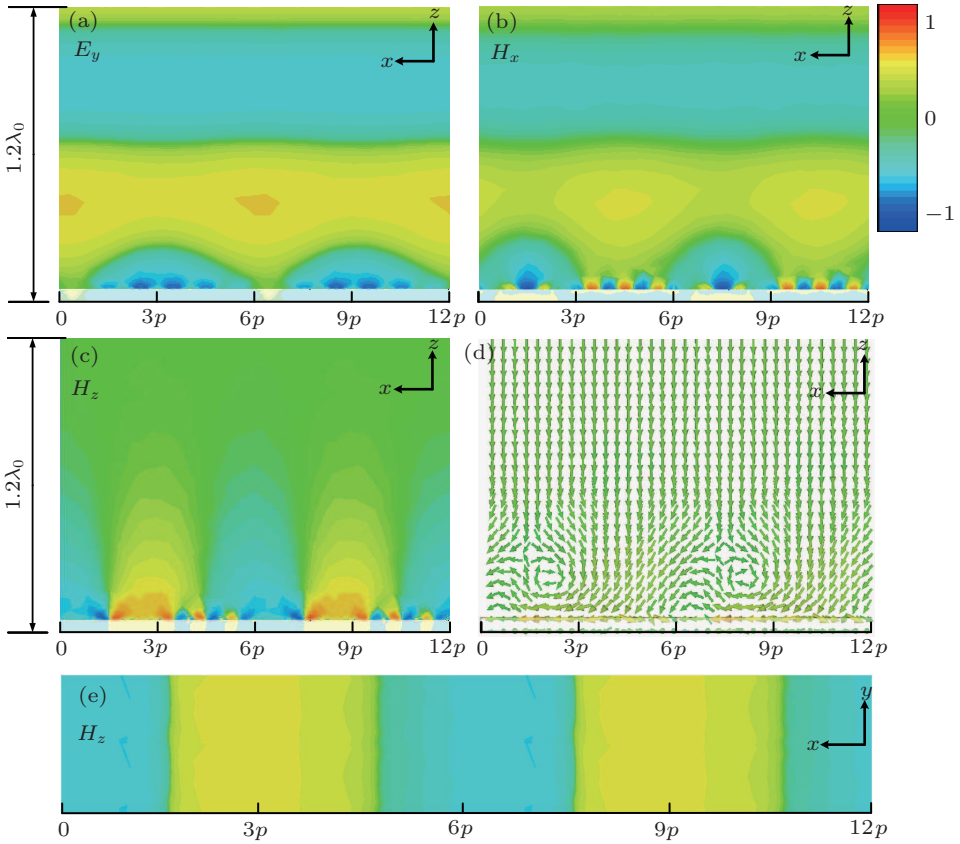


Fig. 8. (color online) (a) The y component of the total electric field. (b) The x component of the total magnetic field. (c) The z component of the total magnetic field in the xz plane. (d) The total power flow in the xz plane at 5.09 GHz under normal-polarized incidence. (e) The z component of the total magnetic field in the xy plane at $z = 5$ mm, where $12p = 2\lambda_{sspp} = 1.6\lambda_0$.

4.2. The measurement results

To verify the simulated results, a 432 mm ×280 mm ($7.2\lambda_0 \times 4.67\lambda_0$) sample was fabricated and the reflectance was measured as shown in Figs. 9(a) and 9(b). The measured reflectance indicates that R_{pp} and R_{nn} are −19.8 dB and −20.7 dB at 4.95 GHz, respectively.

Figure 10 shows the normalized measured radiation patterns under parallel- and normal-polarized normal incidence at 4.95 GHz and 6 GHz. At 4.95 GHz, the scattered field is very small. At 6 GHz, the resonators are with similar reflectance phase, leading to $\xi = 0$. Thus, the gradient metasurface reflects the incident wave back to the source antenna.

The z component of the electric field at parallel-polarized incidence and the z component of the magnetic field at normal-polarized incidence of the coupled spoof SPPs at 4.95 GHz were measured by probes at 5 mm ($0.083\lambda_0$) above the sample and are shown in Figs. 11(a) and 11(b). The sample was illuminated by a plane wave with a width of 80 mm along the y direction. Figure 11 indicates that the incident wave is coupled to spoof SPPs. The measured spoof SPPs were propagating in the x direction with a wavelength of about $6 \times p = 48$ mm. Besides the differences between the simulated and the measured results caused by machining and measurement errors, the results are in good agreement and support the theoretical analysis.

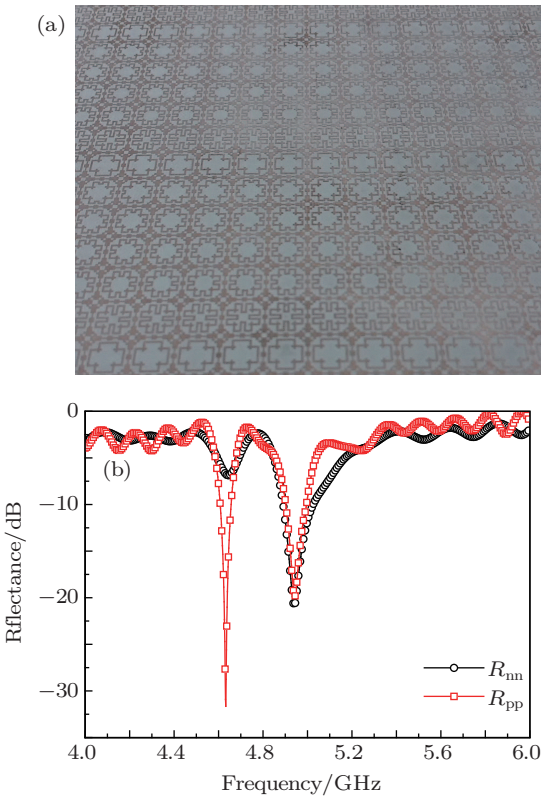


Fig. 9. (color online) (a) A photograph of the fabricated gradient metasurface sample. (b) The measured reflection of the designed gradient metasurface.

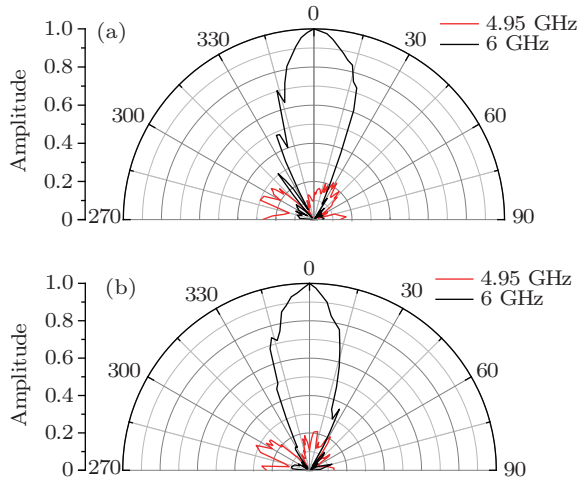


Fig. 10. (color online) The normalized measured radiation patterns: (a) under parallel polarized incidence, (b) under normal polarized incidence.

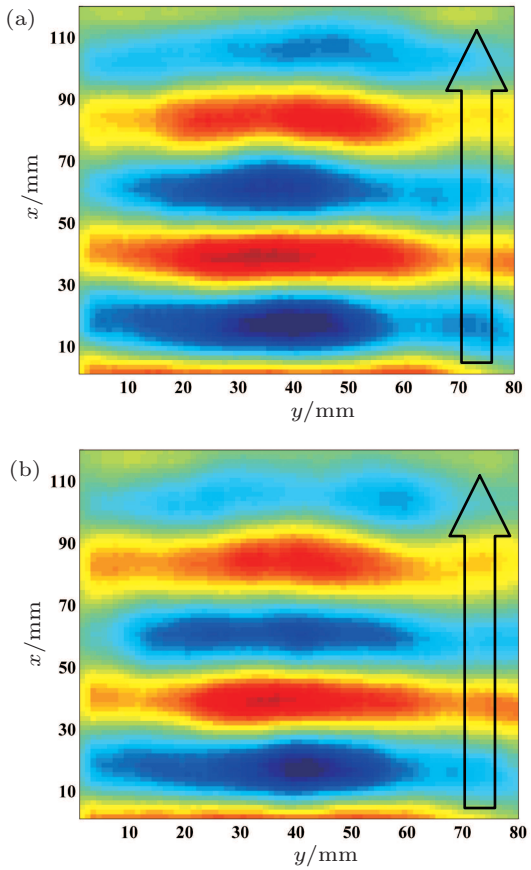


Fig. 11. (color online) The normalized measured fields confined to the surface: (a) the measured z component of the electric field at parallel-polarized incidence; (b) the measured z component of the magnetic fields at normal-polarized incidence.

5. Conclusion and perspectives

A polarization-insensitive unidirectional spoof SPP coupler that can couple both parallel-polarized and normal-polarized incident waves to spoof SPPs is realized using a gradient metasurface. The theoretical analysis gives the field distributions and the average Poynting vector of the coupled spoof SPPs. The measurement results of the designed gradient metasurface conform to the simulated results and also verify the theoretical analysis. This work can be applied to novel microwave devices and antennas and also has a potential value for optical applications.

References

[1] L Li J M, Tang P, Liu W, Huang T, Wang J J, Wang Y Q, Lin F, Fang Z Y and Zhu X 2015 *Appl. Phys. Lett.* **106** 161106
[2] Zhang Y F, Wang H M, Liao H M, Li Z, Sun C W, Chen J J and Gong Q H 2014 *Appl. Phys. Lett.* **105** 231101
[3] Yang J, Xiao X, Hu C, Zhang W W, Zhou S X and Zhang J S 2014 *Nano Lett.* **14** 704
[4] Yu N F and Capasso F 2014 *Nat. Mater.* **13** 139
[5] Yang Y M, Wang W Y, Moitra P, Kravchenko, Briggs D P and Valentine J 2014 *Nano Lett.* **14** 1394
[6] Fratalocchi A, Dodson C M, Genevet P and Verhagen E 2015 *Nat. Nanotechnol.* **10** 11
[7] Li R Z, Guo Z Y, Wang W, Zhang J R, Zhang A J, Liu J L, Qu S L and Gao J 2014 *Opt. Express* **22** 27968
[8] Wang J, Qu S, Xu Z, Ma H, Wang X, Huang D and Li Y 2012 *Photonics and Nanostructures - Fundamentals and Applications* **10** 540
[9] Li Y, Zhang J, Qu S, Wang J, Pang Y, Xu Z and Zhang A 2015 *J. Phys. D: Appl. Phys.* **48** 335101
[10] Estakhri N M and Alu A 2014 *IEEE Antennas Wirel. Propag. Lett.* **13** 1775
[11] Orazbayev B, Mohammadi Estakhri N, Beruete M and Alu A 2015 *Phys.Rev. B* **91** 195444
[12] Wan X, Yin J Y, Zhang H C and Cui T J 2014 *Appl. Phys. Lett.* **105** 083502
[13] Ma H F, Shen X P, Cheng Q, Jiang W X and Cui T J 2014 *Laser Photon. Rev.* **8** 146
[14] Liu X, Feng Y, Chen K, Zhu B, Zhao J and Jiang T 2014 *Opt. Express* **22** 20107
[15] Xu J J, Zhang H C, Zhang Q and Cui T J 2015 *Appl. Phys. Lett.* **106** 021102
[16] Chen B, Shi H, Zhang A and Chen J 2014 *Progress in Electromagnetics Research Symposium, PIERS* **2014** 1383
[17] Wakatsuchi H, Kim S, Rushton J J and Sievenpiper D F 2013 *Appl. Phys. Lett.* **102** 214103
[18] Yao Y, Shankar R, Kats M A, Song Y, Kong J, Loncar M and Capasso F 2014 *Nano Lett.* **14** 6526
[19] Argyropoulos C 2015 *Opt. Express* **23** 23787
[20] Pors A and Bozhevolnyi S I 2013 *Opt. Express* **21** 27438
[21] Zhu B O, Zhao J and Feng Y 2013 *Sci. Rep.* **3** 3059
[22] Shi H, Zhang A, Zheng S, Li J and Jiang Y 2014 *Appl. Phys. Lett.* **104** 034102
[23] Shi H, Li J, Zhang A, Wang J and Xu Z 2014 *Opt. Express* **22** 20973
[24] Zhang Y, Feng Y, Zhu B, Zhao J and Jiang T 2014 *Opt. Express* **22** 22743
[25] Jingwen H, Zhenwei X, Sen W, Xinke W, Qiang K and Yan Z 2015 *Journal of Optics* **17** 105107
[26] Li Z Y, Palacios E, Butun S and Aydin K 2015 *Nano Lett.* **15** 1615
[27] Lin D M, Fan P Y, Hasman E and Brongersma M L 2014 *Science* **345** 298
[28] Su X, Ouyang C, Xu N, Cao W, Wei X, Song G, Gu J, Tian Z, O'Hara J F, Han J and Zhang W 2015 *Opt. Express* **23** 27152
[29] Li Y B, Wan X, Cai B G, Cheng Q and Cui T J 2014 *Sci. Rep.* **4** 6921
[30] Gonzalez-Ovejero D, Martini E and Maci S 2015 *IEEE Trans. Antennas Propag.* **63** 250
[31] Yu N F, Genevet P, Kats M A, Aieta F, Tetienne J P, Capasso F and Gaburro Z 2011 *Science* **334** 333
[32] Yahong L, Xin Z, Kun S, Mei W and Xiaopeng Z 2015 *J. Phys. D: Appl. Phys.* **48** 365301
[33] Zhang K, Ding X M, Zhang L and Wu Q 2014 *New J. Phys.* **16** 103020
[34] Jiang S C, Xiong X, Hu Y S, Jiang S W, Hu Y H, Xu D H, Peng R W and Wang M 2015 *Phys. Rev. B* **91** 125421
[35] Sun S L, Yang K Y, Wang C M, Juan T K, Chen W T, Liao C Y, He Q, Xiao S Y, Kung W T, Guo G Y, Zhou L and Tsai D P 2012 *Nano Lett.* **12** 6223

[36] Aieta F, Genevet P, Yu N F, Kats M A, Gaburro Z and Capasso F 2012 *Nano Lett.* **12** 1702
[37] Ma H F, Wang G Z, Kong G S and Cui T J 2015 *Sci. Rep.* **5** 9605
[38] Pfeiffer C and Grbic A 2013 *Phys. Rev. Lett.* **110** 197401
[39] Yu J B, Ma H, Wang J F, Li Y F, Feng M D and Qu S B 2015 *Chin. Phys. B* **24** 098102
[40] Sun S L, He Q, Xiao S Y, Xu Q, Li X and Zhou L 2012 *Nat. Mater.* **11** 426
[41] Wang J F, Qu S B, Ma H, Xu Z, Zhang A X, Zhou H, Chen H Y and Li Y F 2012 *Appl. Phys. Lett.* **101** 201104
[42] Shi H Y, Li J X, Zhang A X, Jiang Y S, Wang J F, Xu Z and Xia S 2015 *IEEE Antennas Wirel. Propag. Lett.* **14** 104
[43] Huang L L, Chen X Z, Bai B F, Tan Q F, Jin G F, Zentgraf T and Zhang S 2013 *Light-Science & Applications* **2** e70
[44] Pors A, Nielsen M G, Bernardin T, Weeber J C and Bozhevolnyi S I 2014 *Light-Science & Applications* **3** e197
[45] Takayama O, Artigas D and Torner L 2014 *Nat. Nanotechnol.* **9** 419
[46] Lin J, Mueller J P B, Wang Q, Yuan G H, Antoniou N, Yuan X C and Capasso F 2013 *Science* **340** 331
[47] Li Y B, Cai B G, Wan X and Cui T J 2014 *Opt. Lett.* **39** 5888
[48] Wan X, Li Y B, Cai B G and Cui T J 2014 *Appl. Phys. Lett.* **105** 121603
[49] Li Y F, Zhang J Q, Qu S B, Wang J F, Chen H Y, Xu Z and Zhang A X 2014 *Appl. Phys. Lett.* **104** 221110
[50] Kern D J, Werner D H, Monorchio A, Lanuzza L and Wilhelm M J 2005 *IEEE Trans. Antennas. Propag.* **53** 8
[51] Munk B 2000 *Frequency Selective Surfaces: Theory and Design* (New York: John Wiley)